AIAA-91-1532-CP

Multi-Dimensional Schemes for Scalar Advection

Herman Deconinck
Kenneth G. Powell
Philip L. Roe
Robert Struijs

Von Kármán Institute for Fluid Dynamics
Rhode-Saint-Genèse, Belgium
and
Department of Aerospace Engineering
The University of Michigan
Ann Arbor, MI USA

May, 1991

Abstract

Schemes for two-dimensional advection, based on the full advection direction, are derived and tested. The optimal, positive, linear scheme for triangles is presented and discussed. A technique for developing nonlinear schemes for linear problems is put forward, and positive, nonlinear schemes for triangles and quadrilaterals are presented. The linear schemes are based only on the advection direction and the mesh geometry; the nonlinear schemes add solution-gradient information to attain increased accuracy. All of the schemes are compact; the updates can be done on a cell-wise basis, using only the nodes that define that cell. All show a very marked improvement over mesh-aligned first-order upwind differencing, which employs the same stencil.

Introduction

Much of the insight employed in the development of modern-day algorithms for solving advection-dominated problems comes from the equation for one-dimensional advection

$$\frac{\partial u}{\partial t} + a\frac{\partial u}{\partial x} = 0\,. \tag{1}$$

Most schemes for advection-dominated problems in two dimensions are based on applying the one-dimensional schemes along mesh directions; i.e. upwinding based on the projection of the advection direction onto the normal to a cell-face.

The short-comings of this approach are apparent on problems in which the advection direction is not aligned with the mesh. As an example of this, a circular advection field,

$$a(x,y) = y \tag{2a}$$
$$b(x,y) = \frac{1}{2} - x\,, \tag{2b}$$

and boundary conditions given by

$$u(0,y) = 0 \tag{3a}$$
$$u(x,1) = 0 \qquad x \geq \frac{1}{2} \tag{3b}$$
$$u(x,0) = \begin{cases} 0 & x \leq 0.175 \\ 1 & 0.175 < x < 0.325 \\ 0 & 0.325 \geq x < \frac{1}{2} \end{cases}, \tag{3c}$$

yield excessively smeared results when first-order, mesh-aligned upwinding is applied. On the mesh shown in Figure 1, which is a Delaunay triangulation of a relatively uniform point cloud, the input distribution (the left half of the lower boundary) is smeared quite a bit by the time it reaches the outflow (the right half of the lower boundary), as seen in Figure 2.

While high-resolution mesh-aligned schemes give vastly improved results, the schemes presented in this paper, *using the same stencil as the first-order upwind scheme*, give results that are better yet.

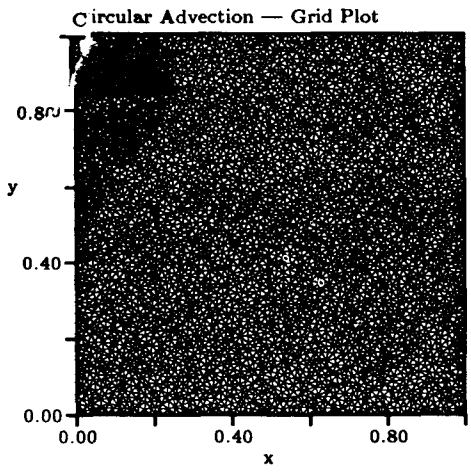

Figure 1: Mesh for Circular Advection Problem

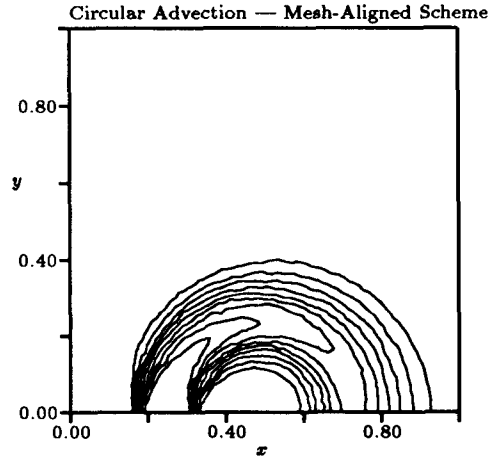

Figure 2: Contours of u for Circular Advection Problem — Mesh-Aligned Upwind Scheme

General Formulation of the Schemes

The equation for two-dimensional advection,

$$\frac{\partial u}{\partial t} + a\frac{\partial u}{\partial x} + b\frac{\partial u}{\partial y} = 0\,, \tag{4}$$

may be solved by any one of a number of finite-difference, finite-volume or finite-element schemes. The schemes described in this paper fall in the broad class of "cell-vertex," or "fluctuation-splitting" schemes, which use conforming finite elments to represent the data, but do not necessarily use the "weak solution/test function" formalism to generate updates [1]. A recent survey of what has been accomplished within a more conventional finite-element framework has been given by Hughes [2]. Many well-known finite-volume and finite-element schemes may be interpreted in the fluctuation-splitting framework. The unknowns, u, are thought of as being associated with nodes in the mesh, and as varying linearly along faces in the mesh. A residual, or fluctuation, for a cell in the mesh may be calculated by integrating equation 4 over a cell, giving

$$\phi_C = \iint_C \frac{\partial u}{\partial t}\,dx\,dy \tag{5a}$$

$$= -\iint_C \mathbf{a}\cdot\nabla u\,dx\,dy \tag{5b}$$

where $\mathbf{a}$ is the advection direction (a, b). By Gauss' theorem,

$$\phi_i = \oint_{\partial C} u\mathbf{a}\cdot\hat{\mathbf{n}}ds \tag{6a}$$

where $\hat{\mathbf{n}}$ is the inward-pointing unit normal to the cell face, and the integral is carried out counter-clockwise. The fluctuation calculation for a triangular cell is depicted in Figure 3.

Making use of the linear representation of u on each face, the boundary integral may be evaluated, giving

$$\phi_C = \frac{u_1+u_2}{2}\mathbf{a}\cdot\mathbf{n}_3 + \frac{u_2+u_3}{2}\mathbf{a}\cdot\mathbf{n}_1 + \frac{u_3+u_1}{2}\mathbf{a}\cdot\mathbf{n}_2\,, \tag{7}$$

where $\mathbf{n}_i$ is the scaled normal to the face opposite the i^{th} node. Using the fact that

$$\mathbf{n}_1+\mathbf{n}_2+\mathbf{n}_3 = 0, \tag{8}$$

Equation 7 may be simplified to give

$$\phi_C = -\sum_{i=1}^{3} k_i u_i \tag{9}$$

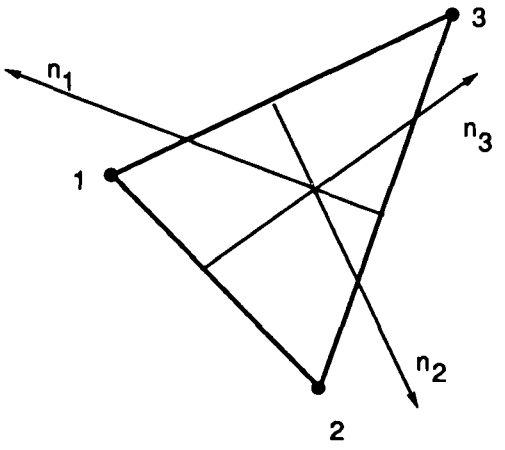

Figure 3: Definition of Cell, Nodes and Normals

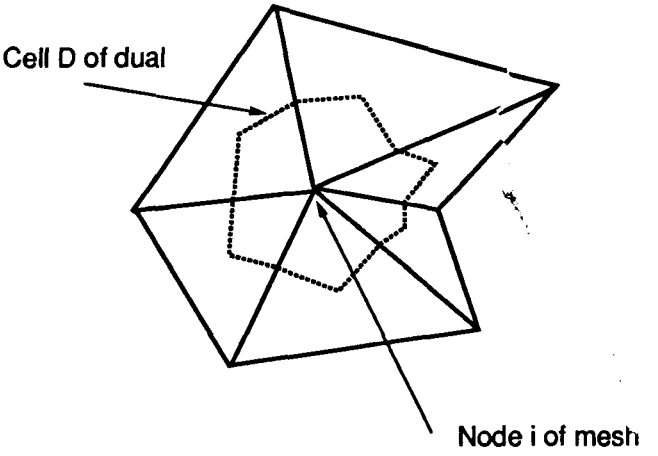

Figure 4: Dual Mesh and Area Associated with Node

where

$$k_i = \frac{1}{2}\mathbf{a}\cdot\mathbf{n}_i \ , \tag{10}$$

and, for example,

$$\mathbf{n}_1 = ((y_3 - y_2),(x_2 - x_3)) \ . \tag{11}$$

Once a fluctuation has been calculated for a cell, it remains to split the fluctuation among the nodes, in order to update the solution at the nodes. The total change in u in the cell, in a time Δt, is $\Delta t\,\phi_C$. This change is scattered to the three nodes of the cell by

$$S_1 u_1 := S_1 u_1 + \alpha_1 \Delta t \phi_C \tag{12a}$$
$$S_2 u_2 := S_2 u_2 + \alpha_2 \Delta t \phi_C \tag{12b}$$
$$S_3 u_3 := S_3 u_3 + \alpha_3 \Delta t \phi_C \tag{12c}$$

where S_i is the area associated with node i (i.e. one-third the area of the triangles having node i as a vertex, or the area of the polygon associated with node i on the median-dual mesh; see Figure 4) and α_i is the fraction of the fluctuation for cell C sent to node i. It is important to note that *each node can get contributions from more than one cell*; for the update scheme defined above, *only cells which share node i as a vertex can send contributions to that node.* To enforce conservation, it is necessary that

$$\sum_i \alpha_i = 1 \tag{13}$$

on each cell.

The two pieces defined above, i.e. the residual calculation step and the distribution step, define a very compact set of schemes — the residual calculation for a cell is based entirely on the nodes of the cell; the fluctuation for that cell is then scattered only to the nodes of the cell. This remains, however, a large class of schemes. The distribution weights (the α_i's) remain to be chosen; the only constraint on them thus far is the conservation constraint, Equation 13.

Linear Schemes and the Advection Direction

The simplest cell-vertex scheme is simply to distribute the fluctuation equally to the nodes of a cell; that is

$$\alpha_i = \frac{1}{3} \tag{14}$$

for triangular cells. (For quadrilateral cells, $\alpha_i = 1/4$). This distribution, in conjunction with the residual calculation step, corresponds to central differencing, or, equivalently, a Galerkin finite-element approach with a lumped mass matrix. The marginal stability of this scheme, and the resulting oscillatory solutions, are well-documented.

A more sophisticated approach is to put some more "physics" into the distribution step; clearly an equidistribution of the fluctuation is inconsistent with the advection problem being solved, and a downwind-biased distribution is more physical. This can result in schemes that are more accurate, and more stable, than the Galerkin scheme. One way to derive such a scheme is to write the change in u at a node as

$$\begin{aligned}\Delta u_i &= \Delta t \iint_D \frac{\partial u}{\partial t}\,dx\,dy + \frac{\Delta t^2}{2}\iint_D \frac{\partial^2 u}{\partial t^2}\,dx\,dy \\ &= \Delta t \iint_D \frac{\partial u}{\partial t}\,dx\,dy + \frac{\Delta t^2}{2}\iint_D \mathbf{a}\cdot\nabla\frac{\partial u}{\partial t}\,dx\,dy\end{aligned}$$

$$= \Delta t \iint_D \frac{\partial u}{\partial t}\, dx\, dy + \frac{\Delta t^2}{2} \oint_{\partial D} \frac{\partial u}{\partial t} \mathbf{a} \cdot \mathbf{n}\, ds \quad (15)$$

where the subscript D denotes the cell in the median dual associated with the node (see Figure 4). The contribution to Δu_i from a triangle C, denoted $(\Delta u_i)^C$ can be shown to be

$$(\Delta u_i)^C = \frac{1}{3}\phi_C + \frac{1}{2}\frac{k_i \Delta t}{S_C}\phi_C \quad (16)$$

where S_C is the area of triangle C. Thus, this scheme, which is a Lax-Wendroff scheme, can be written as a fluctuation splitting scheme with

$$\alpha_i = \frac{1}{3} + \frac{1}{2}\nu_i \quad (17)$$

where

$$\nu_i = \frac{k_i \Delta t}{S_C}\,. \quad (18)$$

The same analysis, on a rectangle C, leads to weights

$$\alpha_{ne} = \frac{1}{4} + \frac{\nu_x + \nu_y}{4} \quad (19a)$$

$$\alpha_{nw} = \frac{1}{4} - \frac{\nu_x - \nu_y}{4} \quad (19b)$$

$$\alpha_{sw} = \frac{1}{4} - \frac{\nu_x + \nu_y}{4} \quad (19c)$$

$$\alpha_{se} = \frac{1}{4} + \frac{\nu_x - \nu_y}{4} \quad (19d)$$

where

$$\nu_x = \frac{a \Delta y \Delta t}{S_C} \quad (20a)$$

$$\nu_y = \frac{b \Delta x \Delta t}{S_C} \quad (20b)$$

This scheme, while more stable and more accurate than the Galerkin scheme, is well known to yield oscillatory results for non-smooth initial conditions (or advection speeds that are a function of u).

Linear Schemes and Positivity

To avoid the oscillations which occur in both the Galerkin and Lax-Wendroff schemes, it is necessary to construct the fluctuation-splitting scheme such that the updated value at a node is bounded by the previous values at some collection of neighboring nodes, i.e.

$$\min_k (u_k^n) \le u_i^{n+1} \le \max_k (u_k^n)\,. \quad (21)$$

A necessary and sufficient condition for this boundedness is that u_i^{n+1} can be written as a convex combination of the u_k^n's;

$$u_i^{n+1} = \sum_k c_k u_k^n \qquad c_k \ge 0 \;\forall\, k. \quad (22)$$

Typically, the values chosen to bound the update at i are all those values that enter in the difference formula for the update of u_i. For the schemes described here, since the residual calculation and distribution steps for a cell are based entirely on the nodal values of u for that cell, it is convenient to base the positivity constraint only on these values as well. The analysis must then be done on a "worst case" basis, which is *more* restrictive than the usual positivity constraint; for each cell contributing to the new value u_i^{n+1}, the fluctuation distribution from that cell is constrained so that it alone does not change u_i^{n+1} by more than some fraction of the change that would take it outside the bounds of the old values at the nodes making up the cell.

The effect of one cell on its three nodes is

$$S_1 u_1 := S_1 u_1 - \alpha_1 \Delta t\, [k_1 u_1 + k_2 u_2 + k_3 u_3] \quad (23a)$$

$$S_2 u_2 := S_2 u_2 - \alpha_2 \Delta t\, [k_1 u_1 + k_2 u_2 + k_3 u_3] \quad (23b)$$

$$S_3 u_3 := S_3 u_3 - \alpha_3 \Delta t\, [k_1 u_1 + k_2 u_2 + k_3 u_3] \quad (23c)$$

For this update to meet the local positivity constraint defined above, it is necessary that the coefficients of each u_i in the right-hand side of each of the above formulas be non-negative. Clearly, the signs of the k_i's are important; since $k_i = \frac{1}{2}\mathbf{a} \cdot \mathbf{n}_i$, the sign of k_i simply denotes whether face i is an inflow face or an outflow face. Since the k_i's must sum to zero for a divergence-free advection field $\mathbf{a}$, there cannot be three inflow sides or three outflow sides. Thus there are only two cases to consider: triangles of type I (one inflow side, and therefore one positive k_i); and triangles of type II (two inflow sides, and therefore two positive k_i's). These two cases are depicted in Figure 5.

For triangles of type I, only one of the k_i's is positive. Say, for example, that k_1 is positive, and k_2 and k_3 are negative. In the equation for the update of u_2, the coefficient of u_1 is then negative, if α_2 is positive. Similarly, in the equation for the update of u_3, the coefficient of u_1 is negative, if α_3 is positive. Therefore, for a postive update of u_2 and u_3, it is necessary that α_2 and α_3 be either zero or negative. The simplest scheme arises from taking them zero. Since the α's must sum to one, this implies that $\alpha_1 = 1$. In the equation for the update of u_1, the coefficients of u_2 and u_3 are non-negative; the coefficient of u_1 is non-negative as long as

$$\frac{k_1 \Delta t}{S_1} \le 1\,. \quad (24)$$

In practice, the constraint

$$\frac{k_1 \Delta t}{S_1} \le \frac{1}{n} \quad (25)$$

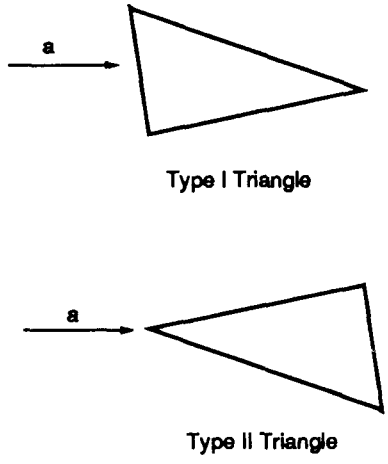

Figure 5: Type I (one inflow side) and Type II (two inflow sides) Triangles

is used, where n is the number of triangles that contribute to the change at that node. For "good" triangulations, it can be shown that $n = 2$. Thus, for the local positivity constraint to be met for a type I triangle, the entire fluctuation can be sent to the node opposite the inflow side, as long as the above time-step constraint is met.

For triangles of type II, two of the k_i's are positive. By similar arguments to those given above, it is easy to show that a positive scheme cannot be constructed, *unless the α_i's depend upon the u_i's*. If the α_i's are taken to be of the form

$$\alpha_i = \frac{\beta_i}{\phi_C} , \tag{26}$$

where the β_i's satisfy

$$\sum_i \beta_i(u_1, u_2, u_3) = \phi_C , \tag{27}$$

the update becomes

$$S_1 u_1 := S_1 u_1 - \beta_1 \Delta t \tag{28a}$$
$$S_2 u_2 := S_2 u_2 - \beta_2 \Delta t \tag{28b}$$
$$S_3 u_3 := S_3 u_3 - \beta_3 \Delta t . \tag{28c}$$

A scheme of this class, for a type II triangle with k_1 and k_2 positive, can be derived by writing

$$\phi_C = -k_1 (u_1 - u_3) - k_2 (u_2 - u_3) \tag{29}$$

which comes from Equation 7 and the fact that the k_i's sum to zero. A positive update based on this form of the residual may be constructed by sending the entire fluctuation to nodes 1 and 2, i.e the two nodes opposite inflow faces;

$$S_1 u_1 := S_1 u_1 - \Delta t\, k_1 (u_1 - u_3) \tag{30a}$$
$$S_2 u_2 := S_2 u_2 - \Delta t\, k_2 (u_2 - u_3) . \tag{30b}$$

This scheme meets the constraint of Equation 27, and is positive as long as

$$\Delta t \leq \min \left[\frac{S_1}{k_1}, \frac{S_2}{k_2} \right] . \tag{31}$$

Again, a worst-case analysis strengthens this to

$$\Delta t \leq \frac{1}{n} \min \left[\frac{S_1}{k_1}, \frac{S_2}{k_2} \right] . \tag{32}$$

The scheme is also linear, a fact that is a happy surprise, since the α_i's are dependent on the u_i's. As written above, however, the update is entirely in terms of the k_i's, which depend only on the triangle geometry and the advection direction. The scheme described above is *the optimal linear scheme* for two-dimensional advection on triangles in the following senses:

- it has the largest time-step of any linear, positive scheme;
- it has, on meshes formed by an optimal subdivision of rectangular meshes, the least truncation error of any scheme in its class [3];
- it has the narrowest stencil of any scheme in its class;
- it is the only positive scheme which gives the exact solution to the advection equation when the advection speed is aligned with a triangle edge.

Results for this scheme, called the N-scheme [3] for its narrow stencil and narrow discontinuities, are shown in Figure 6 for the circular advection problem.

There is one important property that the N-scheme does not possess. It is not guaranteed that data for which all residuals are zero will remain unchanged. This is because the α_i's, as defined in Equation 26, may not be finite, and so the β_i's may be finite even when $\phi_C = 0$. This property, i.e. the preservation of linear solutions (linearity preservation), is possessed by the Lax-Wendroff scheme above. Indeed, it can be shown [4] that linearity preservation is sufficient to ensure second-order accuracy on regular meshes in the steady state.

Moreover, one can prove that *there are no linear schemes of the form in Equation 12d that are both*

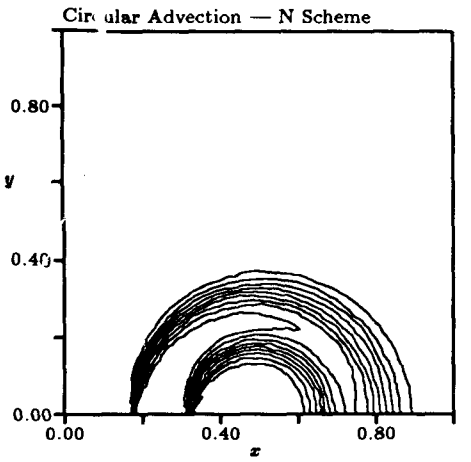

Figure 6: Contours of u for Circular Advection Problem — N Scheme

positive and linearity preserving. This is an analogue of Godunov's famous result for one-dimensional advection, that no linear schemes are both monotone and second-order accurate. This motivates the search for a nonlinear scheme which is both positive and linearity preserving.

NonLinear Schemes and the Solution-Gradient Direction

Improvements in accuracy may be obtained by noting that a function $u(x,y)$ that satisfies

$$\frac{\partial u}{\partial t} + \mathbf{a}\cdot\nabla u = 0 \tag{33}$$

also satisfies

$$\frac{\partial u}{\partial t} + \mathbf{a}^* \cdot \nabla \mathbf{u} = 0\,, \tag{34}$$

where

$$\mathbf{a}^* = \mathbf{a} + \lambda\left(\frac{\partial u}{\partial y}, -\frac{\partial u}{\partial x}\right)\,. \tag{35}$$

Adding this term does not affect the fluctuation ϕ_C calculated for a triangle. It does, however, affect the "apparent" advection speed, and therefore the k_i's. Because these now depend on the data, schemes generated in this way are inherently nonlinear.

It is becoming clear that many previous attempts to generalize from numerical schemes for Equation 33 to more complex advection-dominated problems have come to grief because of the very natural assumption that the wave direction in Equation 33 is $\mathbf{a}/|\mathbf{a}|$, and the wave speed is $|\mathbf{a}|$. A better case can be made for the argument that the wave direction is actually $\nabla u/|\nabla u|$, and the wave speed is $\mathbf{a}\cdot\nabla u/|\nabla u|$. This preserves a convention that all waves propagate normal to their level lines, and makes for a ready generalization to systems of equations [5]. A further advantage is that the wave speed defined in this new way is always *slower* than the usual definition. It therefore allows larger time-steps, particularly close to steady state.

The new k_i^*'s are, in terms of the original k_i's,

$$k_1^* = k_1 + \lambda(u_3 - u_2) \tag{36a}$$
$$k_2^* = k_2 + \lambda(u_1 - u_3) \tag{36b}$$
$$k_3^* = k_3 + \lambda(u_2 - u_1)\,. \tag{36c}$$

If the philosophy taken for the linear scheme is followed, λ may be chosen to maximize the allowable time-step. The resulting scheme may be presented as follows [6]:

```
if (only k_i > 0) then
    α_i = 1
else if (only k_k < 0 ) then
    if( (u_i − u_k) (u_j − u_k) > 0 ) then
        β_i = (u_i − u_k) / (u_i + u_j − 2u_k)
        β_k = (u_j − u_k) / (u_i + u_j − 2u_k)
    else if( (u_i − u_k) φ_C < 0 ) then
        α_i = 1
    else
        α_j = 1
    end if
end if
```

It should be noted that the denominators in the β_i and β_j given above vanish only when the residual vanishes. Thus, numerical problems can be avoided, and the code may be sped up, by simply ignoring any triangles for which the residual falls below some specified threshold. This scheme, which depends nonlinearly on the data, is called the NN (for nonlinear narrow) scheme [6]; other nonlinear schemes with very similar performance are detailed by Deconinck et al [7]. All of them are positive and linearity preserving, and second-order accurate inthe steady state.

The resulting contours for the circular advection problem are shown in Figure 7.

Nonlinear schemes for quadrilaterals can be derived in an analogous fashion. The fluctuation for a square cell may be written in the form

$$\phi_C = \frac{1}{S_C}\left[(a+b)(u_{sw} - u_{ne}) + (a-b)(u_{nw} - u_{se})\right]\,, \tag{37}$$

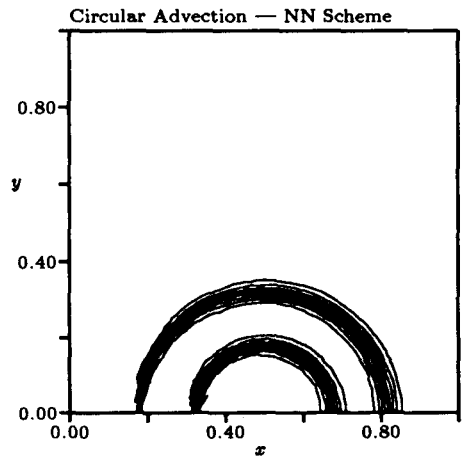

Figure 7: Contours of u for Circular Advection Problem — NN Scheme

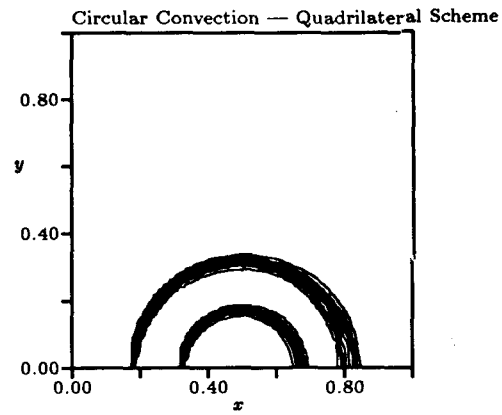

Figure 8: Contours of u for Circular Advection Problem — Quadrilateral Scheme

where sw, se, ne and nw denote the southwest, southeast, northeast and northwest nodes of the cell. As with the triangular case, the advection speeds can be altered, without changing the fluctuation for the cell, by adding a constant λ multiplying a vector normal to the solution gradient. The altered advection speeds (Equation 35) may be written

$$\begin{pmatrix} a^* \\ b^* \end{pmatrix} = -\phi_C \begin{pmatrix} f \\ g \end{pmatrix} . \tag{38}$$

A positive update scheme is then

$$\alpha_{ne} = \begin{cases} 0 & \phi_C (f+g) > 0 \\ \frac{f+g}{2}\left(\frac{\partial u}{\partial x} + \frac{\partial u}{\partial y}\right) & \phi_C (f+g) < 0 \end{cases} \tag{39a}$$

$$\alpha_{sw} = \begin{cases} 0 & \phi_C (f+g) < 0 \\ \frac{f+g}{2}\left(\frac{\partial u}{\partial x} + \frac{\partial u}{\partial y}\right) & \phi_C (f+g) > 0 \end{cases} \tag{39b}$$

$$\alpha_{nw} = \begin{cases} 0 & \phi_C (f-g) < 0 \\ \frac{f-g}{2}\left(\frac{\partial u}{\partial x} - \frac{\partial u}{\partial y}\right) & \phi_C (f-g) > 0 \end{cases} \tag{39c}$$

$$\alpha_{se} = \begin{cases} 0 & \phi_C (f-g) > 0 \\ \frac{f-g}{2}\left(\frac{\partial u}{\partial x} - \frac{\partial u}{\partial y}\right) & \phi_C (f-g) < 0 \end{cases} \tag{39d}$$

In all cases,

$$\begin{aligned} \sum_i \alpha_i &= f\frac{\partial u}{\partial x} + g\frac{\partial u}{\partial y} \\ &= \begin{pmatrix} f \\ g \end{pmatrix} \cdot \nabla u \\ &= -\frac{1}{\phi_C} \begin{pmatrix} a^* \\ b^* \end{pmatrix} \cdot \nabla u \\ &= 1 . \end{aligned} \tag{40}$$

Choosing λ in Equation 35 so as to give the maximum time step yields

$$\begin{pmatrix} f \\ g \end{pmatrix} = \begin{pmatrix} \left(\frac{\partial u}{\partial x}\right)^{-1} \\ 0 \end{pmatrix} \qquad \left|\frac{\partial u}{\partial x}\right| > \left|\frac{\partial u}{\partial y}\right| \tag{41a}$$

$$\begin{pmatrix} f \\ g \end{pmatrix} = \begin{pmatrix} 0 \\ \left(\frac{\partial u}{\partial y}\right)^{-1} \end{pmatrix} \qquad \left|\frac{\partial u}{\partial x}\right| < \left|\frac{\partial u}{\partial y}\right| \tag{41b}$$

The switching that occurs when $|\partial u/\partial x| = |\partial u/\partial y|$ (i.e. when the solution gradient is aligned with a cell diagonal) causes difficulties in convergence. A smoother scheme, defined by

$$\begin{pmatrix} f \\ g \end{pmatrix} = \frac{\nabla u}{\nabla u \cdot \nabla u} \tag{42}$$

yields better results. Contours for this scheme, on a Cartesian mesh with the same number of boundary nodes as the mesh in Figure 1, are shown in Figure 8. For comparison, a second-order mesh-aligned result is shown in Figure 9. This standard scheme, though using a larger stencil than the fluctuation splitting scheme, introduces slightly more diffusion.

A comparison of the distribution of u on the bottom boundary of the domain for the four local schemes (mesh-aligned upwind on triangles, the optimal linear scheme and the optimal nonlinear scheme on triangles, and the nonlinear scheme on quadrilaterals) is shown in Figure 10.

An entirely different approach to constructing compact positive schemes on rectangular grids is presented in [3].

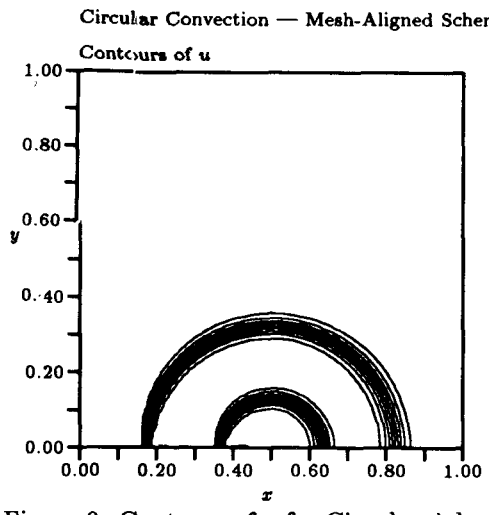

Figure 9: Contours of u for Circular Advection Problem — Mesh-Aligned Scheme

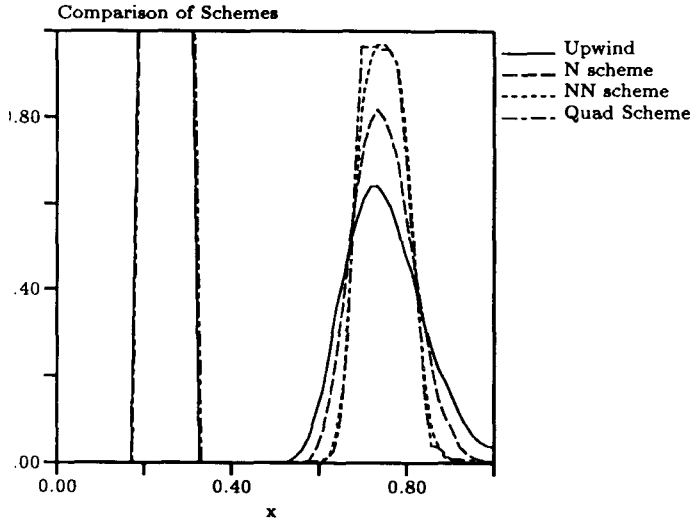

Figure 10: Comparison of Boundary Distribution of u for Circular Advection Problem — Mesh-Aligned Upwind Scheme, Optimal Linear Scheme (N Scheme), Optimal Nonlinear Scheme (NN Scheme), and Quadrilateral Scheme

Nonlinear Problems

Given a nonlinear scalar problem

$$\frac{\partial u}{\partial t} + \frac{\partial}{\partial x} f(u) + \frac{\partial}{\partial y} g(u) = 0 \,, \tag{43}$$

the approach taken is to define an equivalent linear problem within each triangle. Thus, for each cell in the mesh, the problem

$$\frac{\partial u}{\partial t} + a_C \frac{\partial u}{\partial x} + b_C \frac{\partial u}{\partial y} = 0 \tag{44}$$

is considered, where a_C and b_C are constructed so that the residuals on C defined by Equations 43 and 44 are numerically identical.

By definition,

$$\begin{aligned} \phi_C &= \iint_C \frac{\partial u}{\partial t}\, dx\, dt \\ &= -\iint_C \left[\frac{\partial}{\partial x} f(u) + \frac{\partial}{\partial y} g(u) \right] dx\, dy \\ &= -\iint_C \left[\frac{\partial f}{\partial u}\frac{\partial u}{\partial x} + \frac{\partial g}{\partial u}\frac{\partial u}{\partial y} \right] dx\, dy \,. \end{aligned} \tag{45}$$

Assuming that u varies linearly over the cell,

$$\begin{aligned} \phi_C &= -\left[\iint_C \frac{\partial f}{\partial u}\, dx\, dy \right] \frac{\partial u}{\partial x} \\ &\quad -\left[\iint_C \frac{\partial g}{\partial u}\, dx\, dy \right] \frac{\partial u}{\partial y} \,. \end{aligned} \tag{46}$$

Identity between Equations 43 and 44 is therefore ensured by taking

$$a_C \equiv \frac{1}{S_C} \iint_C \frac{\partial f}{\partial u}\, dx\, dy \tag{47a}$$

$$b_C \equiv \frac{1}{S_C} \iint_C \frac{\partial g}{\partial u}\, dx\, dy \,, \tag{47b}$$

where the integrals are computed by assuming that u varies linearly over C. For simple (linear or quadratic) f and g, this is very easy. For the particular nonlinearity involved in the Euler equations, a particular device is available [5].

As an example of a nonlinear advection problem, the equation solved is

$$\frac{\partial u}{\partial t} + \frac{\partial}{\partial x}\left(\frac{u^2}{2}\right) + \frac{\partial u}{\partial y} = 0 \,. \tag{48}$$

Here, the boundary conditions are

$$u(x,0) = 1.5 - 2x \tag{49a}$$

$$u(0,y) = 1.5 \tag{49b}$$

$$u(1,y) = -0.5 \tag{49c}$$

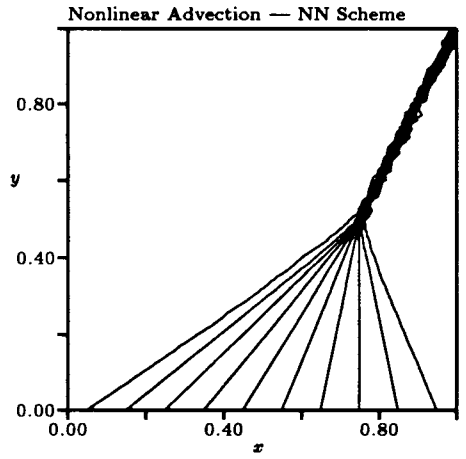

Figure 11: Solution of Nonlinear Problem — NN Scheme

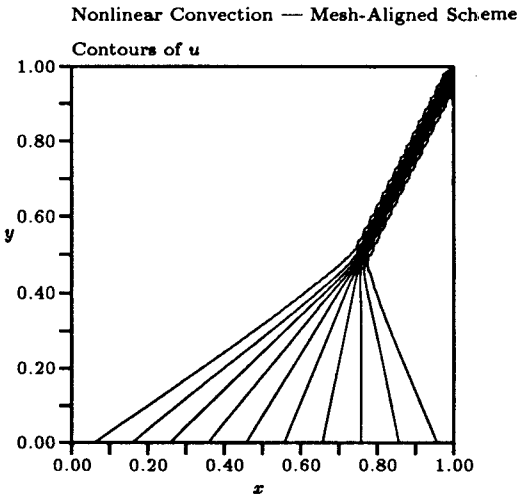

Figure 12: Solution of Nonlinear Problem — Second-order Mesh-Aligned Scheme

Results for the NN scheme are shown in Figure 11; for comparison, results of a second-order mesh-aligned scheme on a Cartesian mesh with the same number of boundary points is shown in Figure 12.

Summary and Remarks

New schemes for solving scalar advection problems have been presented. These improve hugely over first-order upwinding, while retaining very compact stencils. The first level of improvement comes from using the full advection speed, rather than just its projection on the the mesh directions, to motivate the differencing scheme. The second level of improvement comes from using data-dependent, and therefore non-linear, schemes. These exploit the existence of *two* significant directions, by considering the solution gradient direction as well as the advection direction. This second level upgrades the schemes to second-order accuracy when a steady state is reached.

Schemes can be constructed for both structured quadrilateral meshes and unstructured triangular meshes. The results shown here are somewhat better on quadrilateral meshes, but use has not yet been made of the ability to reconnect the nodes of an unstructured mesh so that the triangles become more aligned with the characteristic directions in the problem being solved.

The best results are actually slightly better than those of a state-of-the-art grid-aligned scheme, but this is not the main justification of the new schemes. For scalar advection, a dimension-by-dimension approach is valid at the level of the partial differential equations, so the schemes really address only the numerical error introduced by the dimension-by-dimension approach. For systems of equations, that approach is generally *not* valid for finding discontinuous solutions, so that a physically-motivated approach demands the use of techniques like those given here. The companion paper to this one [5] explains how the bridge from scalar to system case can be constructed.

Although this paper deals entirely with the two-dimensional case, all of the ideas appear to extend to three dimensions quite naturally, although care is needed to choose among the very numerous alternatives that become available. The three-dimensional version of the N-scheme has been worked out by Roe and Sidilkover [8].

References

[1] H. Deconinck, R. Struijs, and P. L. Roe, "Fluctuation splitting for multi-dimensional convection problems: An alternative to finite-volume and finite-element methods," in *Computational Fluid Dynamics*, Von Kármán Institute for Fluid Dynamics, Lecture Series 1990-04, 1990.

[2] T. J. R. Hughes, "Recent progress in the development and understanding of SUPG methods with special reference to the compressible Euler and Navier-Stokes equations," *International Journal*

for Numerical Methods in Fluids, vol. 7, pp. 1261–1275, 1987.

[3] D. Sidilkover, *Numerical Solution to Steady-State Problems with Discontinuities.* PhD thesis, Weizmann Institute of Science, 1989.

[4] T. J. Barth and P. O. Frederickson, "Higher order solution of the Euler equations on unstructured grids using quadratic reconstruction," AIAA Paper 90-0013, 1990.

[5] H. Deconinck, P. DePalma, R. Struijs, P. Roe, and K. Powell, "Progress on multi-dimensional Euler solvers on unstructured grids," in *AIAA 10th Computational Fluid Dynamics Conference*, 1991.

[6] P. L. Roe, "'Optimum' upwind advection on a triangular mesh." ICASE Report 90-75, 1990.

[7] R. Struijs, H. Deconinck, and P. L. Roe, "Fluctuation splitting for the 2-D Euler equations," in *Computational Fluid Dynamics*, Von Kármán Institute for Fluid Dynamics, Lecture Series 1991-01, 1991.

[8] P. L. Roe and D. Sidilkover, "Optimum positive linear schemes for advection in two and three dimensions." Submitted to *Journal of Computational Physics*, 1991.